

Calar Alto ALFA and the sodium laser guide star in Astronomy

D. J. Butler^a, R.I. Davies^a, H. Few^b, W. Hackenburg^a, S. Rabien^a, T. Ott^a, A. Eckart^a, M. Kasper^c

^aMax-Planck-Institut für extraterrestrische Physik,
Postfach 1603, D-85740 Garching, Germany

^bExperimental Physics Dept., National University of Ireland, Galway, Ireland.

^cMax-Planck-Institut für Astronomie, Königstuhl 17, D-69117 Heidelberg, Germany.

ABSTRACT

Adaptive optics (AO) coupled to laser guide star systems is crucial to future ground based astronomical observations. It allows correction of image distortion caused by the Earth's turbulent atmosphere, over a hugely larger fraction of the sky than achieved by using only natural stars. Yet there are still very few such systems producing any sort of scientific results.

ALFA^{*}, now offered on a shared risk basis as a user-instrument at Calar Alto Observatory in Spain, is continuing to improve its performance during closed loop operation on both natural and laser guide stars (LGS). The ability to close the loop on the LGS through thin cirrus cloud (which would remain unseen during normal observing) has the potential to increase the number of nights previously considered suitable for the laser by a factor of about two. In particular, science observations carried out on such a night are described. As part of the TMR[†] network for Laser Guide Stars at Large Telescopes we are studying the distribution of atoms in the mesospheric sodium layer and its' evolution over time. Additionally, a new experiment to provide an on-line monitor of the mesospheric sodium layer has been proposed and the results of a simulation are presented. This study will be of importance to large telescopes with laser stars at good astronomical sites where accurate statistics of the sodium layer are required, both for optimal scheduling of observations and for keeping the wavefront sensor focussed on the LGS.

Keywords: Laser guide star, adaptive optics, sodium layer

1. INTRODUCTION

The MPIA/MPE ALFA instrument, built for the 3.5m telescope at Calar Alto Observatory in Spain, combines adaptive optics with a sodium laser guide star. ALFA uses a natural star for tip/tilt correction and a sodium laser star for higher order correction to improve the Strehl ratio (up to 50%) of stars observed in typical seeing conditions (0.8'' - 1.3'') at near-infrared wavelengths (1 - 2.5 μ m).

Due to the lack of sufficiently bright natural guide stars everywhere in the night sky, a bright, movable reference star is required for AO assisted astronomical observing. The sodium laser star at Calar Alto, created by a 4W cw sodium laser, travels from the coude lab along an optical train to the launch telescope and is focussed on to the mesospheric sodium layer at about 95km. During recent technical time in May 1999, the ALFA team replaced a broken piezo-actuator of a mirror in the laser optical relay train and improved the optical alignment of the laser launch telescope by adjusting the secondary mirror. In addition, the output beam diameter was reduced to 12cm to better match the seeing. As a result of these efforts, the laser spot FWHM was reduced from a typical 2'' - 3'' to 1.7'' in seeing of about 1.2''. As reported in this proceedings¹ no beam wavefront fluctuations on timescales of the order of the atmospheric coherence time were found to influence the laser spot size.

In this paper, we describe our attempts to optimise the performance of the sodium laser guide star coupled to the AO system⁴. We present our latest LGS and tip/tilt star assisted science observations and results of a simulation to monitor the sodium layer using the ALFA laser⁵.

^o

^{*}Adaptive Optics with a Laser For Astronomy

[†]Training and Mobility of Researchers

2. THE LASER GUIDE STAR SYSTEM

2.1. Focussing of Laser on the Shack-Hartmann Sensor

In order to measure accurate wavefront gradients using the LGS, it must be viewed in focus by the SH sensor. Since the NGS is viewed at infinity and the LGS is seen at about 95km at zenith, the SH sensor, which is composed of a 64 x 64 pixel Lincoln Lab CCD with a read noise of $3e^-$ and a gain of $2.5e^- \text{ count}^{-1}$ and a range of remotely changeable lenslet patterns, must be moved to accommodate the different focal positions. In practice, the LGS is focussed as follows.

Firstly, a single lenslet is moved in to the field of view and the position of the brightest pixel is located. Then, centered on this pixel, the ratio of the returned photon flux in a 3x3 pixel grid to that in an annulus from 3 to 9 pixels is calculated. Thus effectively the ratio compares the small to large aperture fluxes, with a higher ratio indicating a better focussed spot. The laser focus position is changed by stepping a motor through a range of positions centered on a typical 'in focus' position. For the ALFA laser, a plateau occurs in the returned photon flux versus motor position plane and so the final motor position is not absolutely critical.

This method is significantly more robust than other schemes for LGS focussing such as FWHM estimation. In particular, when the spot is far out of focus false error estimates can occur due to clumping of photons and algorithms zooming in on a relatively narrow region of the LGS defocus ring. This can then result in the erroneous conclusion that the laser is in focus.

2.2. Focussing of WFS on laser spot

A similar approach to the laser focussing on the sodium layer is planned for focussing the LGS spot on the SH sensor. In this regime the whole sensor is moved through in and out of focus. Keeping the sensor focussed in the LGS is important since any measured defocus – due to changes in the sodium layer itself or simply tracking over long periods of time – will be transferred to the science camera.

2.3. Laser Spot Shape

Recent experiments have shown it is important to have good alignment of the laser beam with the optical axis of the launch telescope. Prior to the May 1999 run, FWHM of 2 to 3 arcsecs was not uncommon. A 12cm laser beam diameter was used to minimize the effect of turbulence on the upward laser propagation through the atmosphere. As shown by Rabien et al¹, any wavefront errors resulting from laser propagation prior to laser launch are negligible. Manual alignment of the secondary mirror allowed the spot FWHM to be reduced to 1.7" as measured on the wavefront sensor. Since the beam diameter is close to or less than r_o at Calar Alto, little high order distortion is expected. Therefore, the spot FWHM limit which is about 1" at the sodium layer should be broadened on the downward link to about 1.56" in seeing of 1.2". Computing the difference (in quadrature) between observation and theory indicates a residual high-order error contribution to broadening of about 0.7". Some tests are planned to determine, whether or not, possible stress on the launch telescope's primary mirror (caused by its supports) contributes to the residual wavefront error.

2.4. Wavefront gradients

Due to the obstruction caused by the secondary mirror some of the hexagonal lenlets in SH sensor are not fully illuminated. The effect of this is to change the measured sub-aperture flux. The error in the centroid estimates needs to be considered by weighting the measured centroids and therefore, the measured wavefront gradients, by the measured photon fluxes. It is important to take these uncertainties into account when calculating the (Zernike) modes to apply to the deformable mirror.

A number of centroiding algorithms are being tested in order to improve the centroid estimates. For now, let us consider two such algorithms, a standard one

$$x_{CG} = \frac{\sum_{i=1}^n x_i \cdot I_i}{\sum_{i=1}^n I_i} \quad (1)$$

where n is the the number of pixels in the x dimension, I_i is the number of counts in pixel i and a weighted threshold centroiding algorithm given by

$$x_{CG} = \frac{\sum x_i \cdot I_i^{1.5}}{\sum I_i^{1.5}} \quad (2)$$

where the counts in each pixel i are weighted by the Poissonian error $I_i^{0.5}$ (ignoring read noise). In the weighted threshold regime, pixels with counts $< 3 \times$ rms readnoise counts of 1.35 are rejected from the calculation.

For an image with a total of 10^3 counts and a peak pixel count of about 50, centroiding algorithms indicate a reduction in rms centroid error from 0.2 pixels to 0.05 pixels using standard and weighted threshold algorithms respectively.

There are 4×16 pixel wide strips in the SH sensor CCD with small sensitivity offsets between them. This phenomenon would tend to add errors to the centroid estimate(s) of some sub-aperture spots by introducing a relative over or under illumination of parts of the spot profile. Although, this problem has not been examined quantitatively, the magnitude of its effect is expected to be small but will be measured and corrected in the near future.

2.5. Observing Plans

Queue scheduling of astronomical programmes for good observing conditions may be an efficient means of maximising the science return. An experiment along these lines will take place this summer at Calar Alto.

3. LIDAR

3.1. Sodium Layer Monitor

In remote sensing experiments a technique that is frequently employed to study the abundances and types of atoms, at any direction in the sky as a function of distance is called LIDAR[‡]. This tool utilises the backscattering of photons from atoms and air molecules by estimating when and how much backscatter occurred using both timing information and the number of returned photons. In practice, it can involve the sending short of duration pulses of light, opening a camera shutter for a known length of time with a known time delay between the time of pulse emission and the shutter opening to collect backscattered photons. Therefore, by calculating the time of flight of the light pulse it is possible to work out when the photons were backscattered and how many particles were involved in the scattering process at a particular distance and volume of air.

As pointed out by recent sodium layer experiments³, the statistics of the long and short term behaviour of the sodium layer have important implications for laser guide star systems. By observing the LGS spot from an off-axis telescope it was found that projected Na layer centroid height variations of the order of 300m occurred in time intervals as short as 30s due to the presence of sporadic layers. Since the aim is to keep the wavefront sensor efficiently focussed on the LGS in order to avoid incorrect defocus terms being applied to the DM, it is now important to obtain measurements of the change in the centre of mass and distribution of sodium atoms along the direction of the laser beam.

The above mentioned LIDAR technique is a strong contender for producing accurate, high temporal and spatial information via an on-line monitoring of the Earth's sodium layer. An experiment to do this at the 3.5m telescope is planned for later this year. The three main components of this experiment are (a) laser modulation (b) data collection and (c) data reduction.

An interesting dilemma exists because although LIDAR requires a pulsed laser as a pre-requisite there is only a cw laser at Calar Alto. In order to remove this hurdle, it is planned to pass the collimated 1mm diameter beam from the main optical bench in the coude lab to an available side bench and to perform amplitude modulation of the beam using an acousto-optical modulator (AOM) placed off-center between two lenses, each with a focal length of 250mm. After the beam has been re-collimated it will be returned to the optical train going to the launch telescope. As will be described later a simple regime of short, isolated pulses is not time efficient. A pseudo-randomly encoded pulse sequence will be employed and will be generated using a pulse generator to drive the AOM. By recording when an out-going pulse is created with the time-tagged groups of backscattered photons it will be possible to calculate the time of flight of photons and therefore determine the altitude from which they were backscattered. A schematic of the proposed laser modulation set-up is shown in figure 1. Since the AOM produces a first order or a zero order output beam depending on whether an RF signal is applied or not, the on/off state of the out-going laser is determined by using only one of AOM output beams. Here, the first order beam is sent to the launch telescope because it is expected to have a zero power level when the laser is in the 'off' state while the first order beam will have a minimum power (in its 'off' state) of 10% of the total power.

In order to obtain the data with the maximum signal to noise ratio, a fast, highly efficient photon-counting detector is required. In collaboration with NUI, Galway, we plan to install a photon counting camera, an APD (Avalanche Photo-Diode) with a 200 μm aperture coupled to some pre-optics for spot minification, at the F/10 focus in the ALFA box. The APD should have a low dark count rate (< 1000 cps) and a quantum efficiency $> 50\%$ at 589nm. The data from the APD will be fed in to a multi-channel

[‡]Light Detection And Ranging

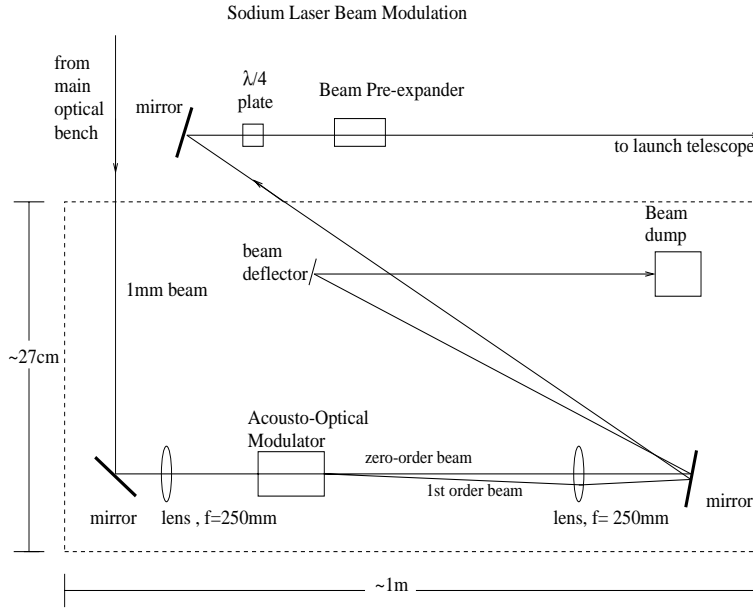


Figure 1. The proposed modulation of the ALFA laser is shown in the dashed box.

scaler (MCS), that can record electronic events occurring in time intervals as short as 125ns and from there it will be saved to a computer hard-disk for processing. Some signal-to-noise calculations were performed to determine if the experiment was feasible in the presence of a bright moon at Calar Alto with a laser star of magnitude $V = 10$ and whether or not a sodium filter is necessary. The conclusion is that sufficient S/N (> 10) is achievable without a filter using instrument and laser modulation parameters listed in the LIDAR simulation section. The drawback of an interference filter is that peak transmission is about 50% and it would cut down the LGS flux as well as the sky background. The set-up for detecting the photons is not trivial and a number of problems are envisaged. In particular, accurate alignment of the LGS beam with the APD will require some consideration.

3.2. Simulation

A simulation was performed to investigate the ability of the proposed LIDAR experiment to reconstruct a useful estimate of the sodium layer's shape. Figure 2 shows the results of a simulation.

The top panel shows the fictitious model sodium layer profile from 90km to 100km altitude with two broad gaussian profiles and a narrow one representing a sporadic sodium layer. A model sporadic layer was included because we wish to examine sensitivity to the detection of sporadic sodium layers with 'widths' of less than about 400m. Given a $0.5\mu\text{s}$ pulse, the model Na profile can be rebinned into 150m bins and this is plotted in the second panel. We see that binning clearly reduces the height resolution achievable.

Given an output laser power (P_{out}) of 2.0 W, an atmospheric transmission (T) of 0.6 at 589nm, Na column density (N_{col}) = 3×10^{13} atoms m^{-2} , cross-section, $\sigma = 8.8 \times 10^{-16}$ m^{-2} we can estimate the expected returned photon flux from a pseudo-random

sequence of circularly polarized, square-wave, sodium laser pulses of duration $\delta t = 0.5 \mu\text{s}$, with 50% on and off. In addition, with 66 Na sub-levels considered in a sodium layer centered at about 95km, the average number of photons per m^2 (N_{ph}), before the telescope, in each $0.5\mu\text{s}$ time bin is

$$N_{ph} \approx \frac{1.2 \cdot P_{out} \cdot T^2 \cdot \sigma \cdot \delta t \cdot \langle N_{col} \rangle}{8 \cdot \pi \cdot H^2 \cdot h \cdot \nu_{589nm}} \quad (3)$$

where $\langle N_{col} \rangle$ is the mean sodium column density in 150m sub-layers (taken here to be 0.18×10^{13} atoms m^{-2}), h is planck's constant and ν_{589nm} is the frequency.

If we now consider a pseudo-random sequence of pulses using the above parameter values, scaling the mean sub-layer column density according to the binned Na profile amplitude (2nd panel) in each sub-layer and include Poisson noise but exclude sky counts, we obtain the returned photon flux shown in the third panel. Here, each $0.5 \mu\text{s}$ bin is joined by a line.

Now, by doing a normalised cross-correlation of the single pseudo-random pulse sequence with the returned flux in $0.5 \mu\text{s}$ bins we get the graph in the bottom panel. So, given 66 sub-layers, each of height 150m, the minimum width estimate that can be made of a sporadic layer detection is between 150m and 300m. It can be seen in the bottom panel that the sporadic layer was recovered by the cross-correlation but is broadened from a FWHM of about 150m to 150m - 200m. Since the pulse sequence considered here is 5000 ($0.5\mu\text{s}$) bits, longer sequences (eg 16kbit) will reduce the bin to bin fluctuations in the cross-correlation output, thereby improving our interpretation of the recovered sodium layer profile. Repeating the pulse sequence and combining them will improve the S/N in each time bin.

The simple conclusion is that estimate of structure of the Na layer can be recovered from the LIDAR experiment and given $0.5\mu\text{s}$ pulses sporadic layers of FWHM < 300 m should be detectable.

Finally, we can estimate the average photon fluxes that may be detected. If the primary and secondary mirror reflectances are 0.85 each, tip/tilt mirror reflectance of 0.8, an APD quantum efficiency of 50%, effective collecting area = $9m^2$, then given very good sky subtraction, an average return of 0.34 photons per $0.5 \mu\text{s}$ is expected given a single pulse sequence of length $0.25ms$. So, repeating the pulse sequence 1000 times and combining each of them gives about 340 photons per $0.5 \mu\text{s}$ bin.

4. RESULTS

4.1. NGC 6764

One of the prime reasons for using a laser guide star is that it allows sharp images to be obtained of extra-galactic objects, most of which do not lie close to bright stars, almost anywhere on the sky. For example, diffraction limited imaging of nearby active galactic nuclei (AGN) allows the dynamics and physical processes occurring on small spatial scales (less than 10pc at a distance of 10Mpc) to be studied by separating out the true nucleus from much of the surrounding stellar population. Similarly, studies of close starbursts can resolve individual star clusters in the core, revealing information about their stellar content (age, mass, size, etc.). For high redshift galaxies it becomes possible to measure and compare the amount of light in the galaxy nucleus and disk: at $z = 3$, $1'' = 6\text{kpc}$, so seeing-limited observations of galaxy nuclear colours will inevitably be seriously contaminated by disk emission.

NGC 6764 is a spiral galaxy at a distance of 32Mpc, classified as a low-ionization nuclear emission-line region (LINER). In this case the line ratios appear to result from a combination of starburst and wind, and there is a prominent 466nm Wolf-Rayet emission feature in the nucleus indicative of very recent massive star formation². The aim was to resolve the nucleus and determine whether the starburst is occurring in several compact clusters and whether star formation has occurred sequentially over different regions in the nucleus. However, observations were restricted by technical problems with the camera.

There are two important benefits of using a sodium laser and observing in the infrared. One is that the LGS can be located in the direction of the target galaxy. Because the wavefront reference is then on-axis, it allows a maximum high-order correction to the science object; something that is usually not feasible with natural stars. The second is that the LGS will not be detected in the near-IR camera – a serious difficulty for optical observations, requiring careful high-speed gating of the LGS and science exposures. Additionally, since stars radiate over a wide spectrum, having a bright NGS close to a faint galaxy would require careful subtraction of the PSF wings, significantly reducing signal-to-noise in the galaxy.

In May 1999, NGC 6764 was observed in the K-band using an AO + tip/tilt star + LGS in seeing of about 0.93 arcsec as measured from an open loop image. In figure 3, we can see difference in compactness of the two stars in the lower left corner

and the galaxy at the upper right of the open loop (uncorrected) image (left) and the closed loop (corrected) image (right). While the laser was pointed at the galaxy nucleus, the $V=14.8$ star used for tip-tilt correction, lies 42 arcsec distant. The galaxy is too faint and the star is too far away for either to be used as a reference for high order correction; this observation could only be achieved using the laser. An even fainter ($V > 16$ mag) PSF comparison star lies between the two, 25 arcsec from the galaxy.

The tip-tilt correction made no measurable difference. Probably this is because the star was quite distant and also rather faint (at our limit) so the frame rate was only 10 Hz, and the bandwidth much less. However, the LGS did provide a good improvement, increasing the peak intensity on the star by a factor of 2.8 and reducing the FWHM to 0.55 arcsec (see the profiles shown in figure 4). At this image resolution the galaxy nucleus is clearly resolved, having a FWHM of 1.26 arcsec. Taking in to account the FWHM of a natural star, an intrinsic size of 1.13 arcsec, equivalent to 175 pc is estimated. At the diffraction limit of the 3.5-m telescope in the K-band (~ 0.15 arcsec, equivalent to 23pc) we would be able to clearly map the intensity distribution across the nucleus.

In figure 5, an example of a 0.01s 3×3 lenslet array sub-aperture image of the LGS from the May 1999 observation (left) is compared with one from a previous observation taken in 1998 (right). The recent sub-images are more compact with less halo noise, so that it is now much more successful and reliable compared to previous attempts to close the AO loop on the LGS. The central spot in the right hand image is a result of AO mis-alignment such that the central obscuration did not line up with the middle subaperture.

The peak counts, in the left image are 60–70 per pixel with FWHM of about 3.5 pixels and total counts of about 1200. Due to the presence of faint cirrus scattering light from the laser beam and reducing the LGS intensity, the 3×3 lenslet array was chosen instead of the usual 5×5 array to ensure a maximum signal-to-noise ratio.

The problem of such clouds can be seen in figure 6 where the LGS was imaged through cirrus clouds. It is an extremely important step that we are now able to lock the AO loop in these conditions, with the result that the number of nights suitable for AO+LGS observations is expected to increase by a factor of about two at Calar Alto.

5. FUTURE

The ALFA laser system will continue to be improved via work on the problem of spot size degradation from theory limits and improvements in accuracy of wavefront gradient measurements. In addition, the near IR science that has started to come from its use is expected to increase significantly in the near future.

ACKNOWLEDGEMENTS

The MPIA/MPE team thanks the Calar Alto staff for their assistance. DJB, RID and HF acknowledge the support of the TMR programme for Laser Guide Stars on 8m Class Telescopes under contract ERBFMRXCT 960094. N. Ageorges is thanked for careful reading of a near final draft of this paper.

REFERENCES

- ¹ S. Rabien, R. Davies, W. Hackenburg, A. Eckart, T. Ott, “Beam quality and polarization analysis of the ALFA Laser at Calar Alto and the influence on brightness and size if the laser guide star”, Proc. SPIE, 3762, Paper 45, 1999
- ² A. Eckart, M. Cameron, TH. Boller, A. Krabbe and M. Blietz, “The Starburst in the Wolf-Rayet Nucleus of the Liner NGC 6764”, ApJ, 472, 588-599, 1996

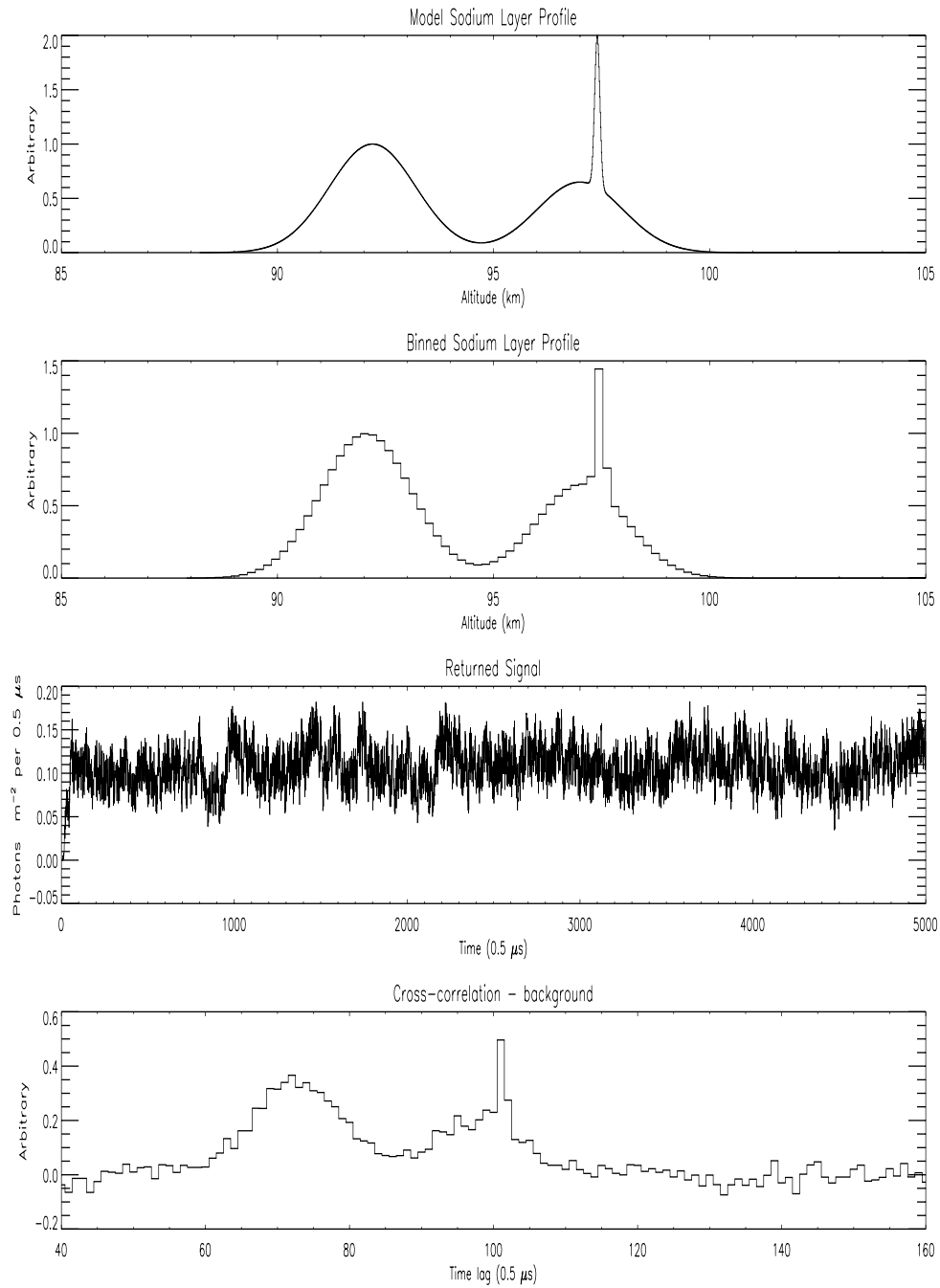


Figure 2. Top to bottom: Model Sodium Layer Profile; Na layer sampled and binned in 150m intervals; Returned signal in $0.5 \mu\text{s}$ time bins from a 5000 bit pseudo-randomly encoded sequence of $0.5 \mu\text{s}$ square-wave on/off states; normalised cross-correlation of returned signal with out-going sequence (minus the the background).

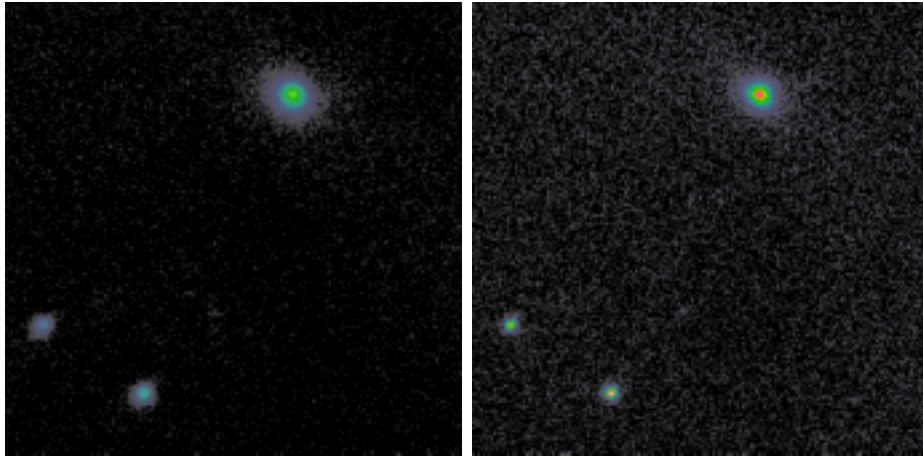


Figure 3. Left: 10x10s uncorrected 34" x 34" arcmin K band image of NGC 6764 at top right. Right: 2x10s corrected K band image with the laser pointed at the galaxy, for correction of high order modes and the tip/tilt star at 42" away, lies off the image to the bottom left.

³ C. M. M. O' Sullivan, R. M. Redfern, N. Ageorges, H. -C. Holstenberg, W. Hackenberg, S. Rabien, T. Ott, R. Davies and A. Eckart, "The Mesospheric Sodium Layer at Calar Alto, Spain", *Exp. Astronomy*, in press, 1999

⁴ S. Hippler, A. Glindemann, M. Kasper and P. Kalas and R. R. Rohloff and K. Wagner and D. Looze, "ALFA: The MPIA/MPE adaptive optics with a laser for astronomy project", *Proc. SPIE*, in *Adaptive Optical System Technologies*, 3353, Paper 05, 1998

⁵ A. Glindemann, S. Hippler, M. Kasper, P. Kalas, R. R. Rohloff, K. Wagner, D. Looze and W. Hackenburg, "ALFA - The laser guide star adaptive optics system for the Calar Alto 3.5m telescope", in *Laser Technology for Laser Guide Star Adaptive Optics Astronomy* (ESO), 120-125, 1997

NGC 6764

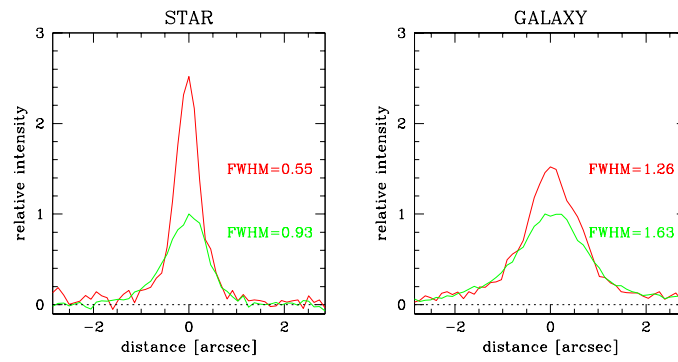


Figure 4. Open and closed loop profiles of NGC6764 (right) and the star 25'' distant (left) are plotted. The LGS was pointed at the galaxy and the tip/tilt star is 42'' away.

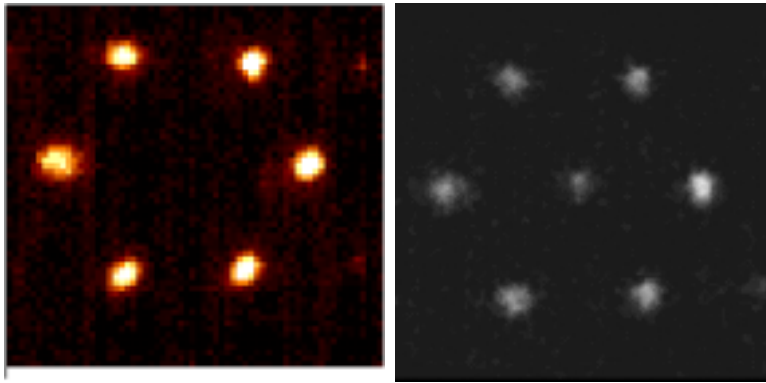


Figure 5. Left: 3x3 lenslet array sub-aperture images of the laser star recorded at 100Hz in May 1999. Right: 3x3 lenslet array of LGS spots taken at 60Hz in 1998. The central spot is due to AO mis-alignment and the central obscuration not covering the middle sub-aperture.

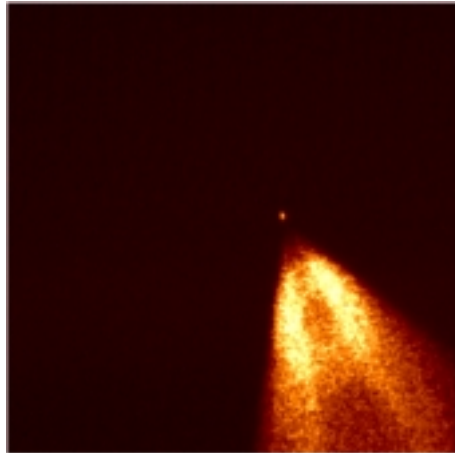


Figure 6. TV guider image of the LGS spot (top) and the laser plume resulting from back-scattered light from thin altitude clouds.